# Laser Ablation Dynamics of a Poly(methyl methacrylate) Film Doped with 5-Diazo Meldrum's Acid

**Hisashi Fujiwara,† Yoshinori Nakajima, Hiroshi Fukumura,* and Hiroshi Masuhara***

*Department of Applied Physics, Osaka University, Suita 565, Japan*

*Received: July 20, 1994; In Final Form: April 17, 1995*[⊗]

The 248 nm ablation of poly(methyl methacrylate) (PMMA) doped with 5-diazo Meldrum's acid (DM) has been investigated by measurements of etch profile, transient absorption spectra, and transient absorbance at 248 nm. There were three fluence regions with respect to characteristic morphological changes of the polymer film; no morphological change, an elevation of the film surface (swelling), and etching were observed in the low, medium, and high fluence regions, respectively. The photodecomposition of DM into the ketene was confirmed by transient absorption spectroscopy, and its yield was determined to be 0.62. The results obtained by transient absorption spectroscopy made it possible to simulate the photodecomposition dynamics of DM, and the amounts of the absorbed energy and the photodecomposition products were estimated. On the basis of the obtained results, it is concluded that the amount of the absorbed energy governs ablation; namely, thermal processes are dominant although DM photodecomposes with a high quantum yield. The cyclic multiphotonic absorption by the ketene is discussed.

## 1. Introduction

Most of the studies on laser ablation of polymers have concerned its application to microfabrication, because it has the following advantages: (1) the low divergence of a laser beam allows the selective removal of polymer surface with high spatial resolution; (2) laser ablation has a "self-developing" character and thus can be a one-step lithographic technique; (3) in contrast to ion plantation/sputtering and electron beam processes, laser ablation can be applied in air or liquid.[1] However, laser ablation is due to photoreactions caused by extremely intense laser excitation and is one of the most interesting photochemical and photophysical phenomena.[2] For example, the intense excitation may cause simultaneous or stepwise multiphoton absorption, mutual interactions between excited states, and successive excitation of the produced intermediates. The relaxation of the absorbed photon energy leading to ablation includes bond breaking, heat generation, and the ejection of the fragmented polymer. Thus, the laser ablation mechanism is an important and interesting subject on laser photochemistry and photophysics of condensed matters.

In the past decade, many polymers have been studied for laser ablation: poly(methyl methacrylate) (PMMA), polystyrene, polyimide, poly(ethylene terephthalate), and so on. Not only those neat polymers but also doped polymers have been frequently used in ablation studies.[3−19] Doped polymer films have characteristic advantages: (1) we can sensitize, by using an appropriate dopant, the film which has no or little absorption coefficient at the excitation laser wavelength; (2) the careful choice of a dopant whose photophysical and photochemical properties are well-known enables us to discuss the mechanism of doped polymer ablation from desired viewpoints. There have been two theoretical models for interpreting doped polymer ablation: photothermal[3−15] and photodecomposition mechanisms.[16−19] In the photothermal mechanism, a dopant works as a molecular point heater.[10−14] Namely, it absorbs excitation photons, converts their energy to its vibrational energy, and then heats the surrounding matrix polymer through the vibrational cooling. The heated polymer decomposes thermally, which induces ablation. In this mechanism, the total amount of the absorbed energy governs ablation. In the photodecomposition mechanism, on the other hand, a dopant molecule absorbs excitation photons and then decomposes to yield gaseous products which exert high pressure to the surrounding matrix polymer. It induces fragmentation of the polymer and then expels the fragments, which results in ablation. In this mechanism, the amount of the photodecomposition products governs ablation. Two key parameters, the amounts of the absorbed energy and the photodecomposition products, are crucial in discussing the mechanism and are examined by choosing 5-diazo-2,2-dimethyl-1,3-dioxane-4,6-dione (5-diazo Meldrum's acid, DM) as a dopant in poly(methyl methacrylate) (PMMA) film. DM is one of the representative photoactive molecules, and hence it is suitable for studying the photodecomposition mechanism of doped polymer ablation.

DM in PMMA photodecomposes with a high quantum yield when irradiated with a KrF excimer laser pulse.[20] We obtained the amount of the absorbed energy simply by monitoring the transmitted 248 nm laser pulse, while it was not simple to estimate the amount of the photodecomposition products. The intermediates could include carbene (**1**), oxirene (**2**), ketene (**3**), and ketene hydrate or carboxylic acid enol (**4**) as shown in Scheme 1,[21] and the produced $N_2$ molecule may be the "driving gas" in the photodecomposition mechanism. Applying transient absorption spectroscopy to the films, the photodecomposition dynamics was investigated and the amount of the photodecomposition products was estimated.

On the basis of these results, we discuss the fluence dependence of the etch depth, the thickness dependence of the morphological changes, and the nature of dopant sensitization. It is also shown that the photoabsorption by the intermediates produced from the dopant has an important role in laser ablation.

## 2. Experimental Section

**Samples.** Dichloromethane (99.5%, Nacalai Tesque), methyl isobutyl ketone (99.5%, Wako), isopropyl alcohol (99%, Dojin),

† Present address: Department of Information Machines and Interfaces, Hiroshima City University, 150-1 Ozuka, Numata-cho, Asa-minami-ku, Hiroshima 731-31, Japan.

⊗ Abstract published in *Advance ACS Abstracts,* June 15, 1995.

0022-3654/95/2099-11481$09.00/0 

**SCHEME 1**

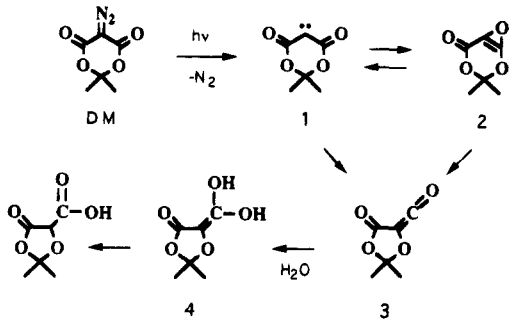


**TABLE 1: Abbreviation, Thickness, and Absorption Coefficient of Examined Sample Films**

| abbrev[a] | preparation method | film thickness $d$ ($\mu$m) | absorption coeff[b] $\alpha$ ($cm^{-1}$) |
|---|---|---|---|
| DM(0.61 M)/PMMA-S | spin coating | 1.8 | $1.3 \times 10^4$ |
| DM(0.36 M)/PMMA-S | spin coating | 1.6 | $7.9 \times 10^3$ |
| DM(0.15 M)/PMMA-S | spin coating | 1.5 | $5.6 \times 10^3$ |
| DM(0.14 M)/PMMA-C | casting | 36 | |
| PMMA-S | spin coating | 1.5 | $1.7 \times 10^2$ |
| PMMA-C | casting | 35 | $1.8 \times 10^2$ |

[a] The concentration of DM is indicated in parentheses. The letters S and C denote spin-coated and solvent-cast films, respectively. [b] The value at the excitation wavelength (248 nm).

and DM (Tokyo Kasei) were used as received. PMMA (polymerization degree $\approx$ 1000, supplied by Kuraray Co. Ltd.) was purified by reprecipitating it from benzene solution with methanol several times. PMMA with or without DM was dissolved in dichloromethane. Sample films were prepared on a quartz plate from the solution either by spin coating or by solvent casting. Spin-coated films were dried under vacuum in an oven; the temperature was gradually increased to 110 °C in 1 h, kept at this temperature for 15 min, and then cooled slowly overnight. Solvent-cast films were dried for several hours under vacuum at room temperature. We prepared six types of the films whose abbreviations and parameters are listed in Table 1.

**Laser Irradiation.** A KrF excimer laser (248 nm, Lambda Physik, EMG201MSC) was used for irradiation of the films. The laser pulse width was about 30 ns. The laser pulse was trimmed through an aperture and focused normally onto a film surface by using a quartz lens ($f$ = 20 cm). The laser fluence was adjusted by placing partially transmitting laser mirrors in front of the laser output. In all measurements except for one to determine the quantum yield of the photodecomposition of DM, we irradiated a fresh film surface to avoid a complication arising from interactions between the irradiated surface and the successive laser pulses.

**Depth Measurement.** The surface profiles of the irradiated films were measured with a depth profiler (Sloan, Dektak). In the case of DM(0.61 M)/PMMA-S, the profiles were also measured after development. The developer was a mixture of methyl isobutyl ketone and isopropyl alcohol (3:1), and the development was done by soaking the irradiated films in it for 1 min.

**Transient Absorption Spectral (260−450 nm) Measurement.** Transient absorption spectra of the DM-doped PMMA was measured by using a pulsed 300 W xenon lamp (Wakom, KXL-300F) as a monitoring light source. The monitoring light was incident at 45° on the film, and the transmitted light was passed through a polychromator (Jovin Yvon, HR-320) and then detected by a streak camera system (Hamamatsu, C2830 and C3140). The streak images of delay time × wavelength were obtained by averaging five measurements, from which spectra and their rise-and-decay curves were obtained.

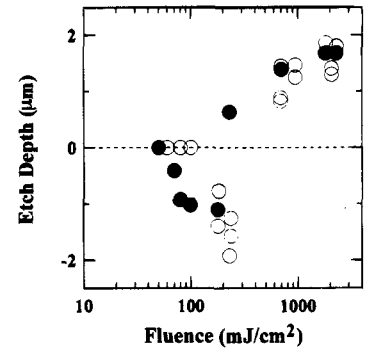


**Figure 1.** Fluence dependence of the etch depth of DM(0.36 M)/PMMA-S (○) and DM(0.61 M)/PMMA-S (●).

**Transient Absorbance at the Laser Wavelength (248 nm).** Transient absorbance of the film at the excitation wavelength was measured by using two pin photodiodes (Hamamatsu, S1722-02).[8] A small part of the incoming laser pulse was separated by a quartz plate beam splitter and detected by the first photodiode. The transmitted laser pulse was simultaneously detected by the second photodiode. The signals from two photodiodes were recorded on a digitizing oscilloscope (Hewlett-Packard, HP54510A). Time-integrated or time-resolved absorbance was calculated on a microcomputer. Time-resolved absorbance obtained either at the beginning or at the end of the laser pulse contained a relatively large uncertainty because the signals from the photodiodes were small.

## 3. Results

**Etch Depth.** We prepared six kinds of PMMA films to investigate the dependence of laser ablation on the DM concentration and the film thickness. Each film showed morphological changes above a certain threshold fluence, and the irradiated surface was not smooth. In some cases there were fibrous residues on the surface, especially near and at the edge.

We first measured the etch depth of each film mainly to obtain its general fluence dependence, because the dependence is necessary for discussing the ablation mechanism as can be seen in the Discussion. Figure 1 shows the fluence dependence of the etch depth of DM(0.61 M)/PMMA-S and DM(0.36 M)/PMMA-S. The negative values of the ordinate indicate an elevation of the surface,[5,22] which was termed "swelling" by Fukumura *et al.* In this paper, we use the word "swelling" only to mean an elevation of the surface, while we use the word "etching" only to mean a dropping of the surface. The threshold of the swelling of DM(0.61 M)/PMMA-S was 40−50 mJ/cm$^2$, and it was smaller than that of DM(0.36 M)/PMMA-S (120 mJ/cm$^2$); the threshold of the swelling decreased with an increase in the DM concentration. The same tendency was observed for the etching threshold; the value was 200 mJ/cm$^2$ for DM(0.61 M)/PMMA-S and 400 mJ/cm$^2$ for DM(0.36 M)/PMMA-S. The maximum amounts of the swelling, however, showed the opposite tendency; the values were about 1 $\mu$m just below 200 mJ/cm$^2$ for DM(0.61 M)/PMMA-S and about 2 $\mu$m around 200 mJ/cm$^2$ for DM(0.36 M)/PMMA-S. In the case of DM(0.61 M)/PMMA-S, a switch from the swelling to the etching was observed around 200 mJ/cm$^2$, and a similar switch was previously observed in the case of porphyrin-doped polymer ablation.[5] Above 1000 mJ/cm$^2$, most of the film within the irradiated area was removed for both films.

Both swelling and etching of the films depend not only on the DM concentration as in Figure 1 but also on the film

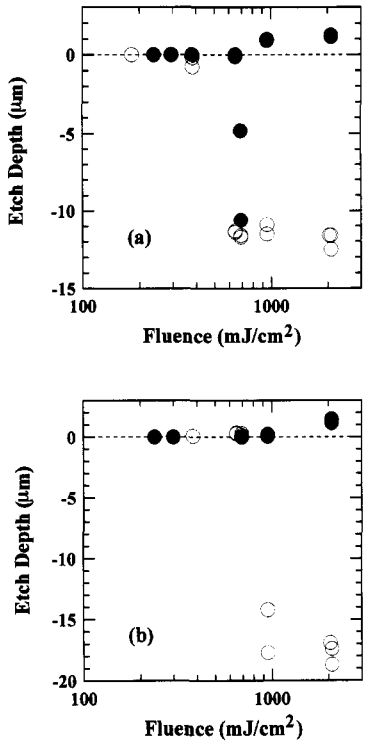


**Figure 2.** Comparison of the fluence dependence of the etch depth of the thin spin-coated films and that of the thick cast films. (a) The closed and open circles show the dependence of DM(0.15 M)/PMMA-S and DM(0.14 M)/PMMA-C, respectively. In the case of DM(0.15 M)/PMMA-S, a considerable swelling suddenly occurred just above the threshold, and thus the data there should contain a relatively large uncertainty. Those data are distinguished by gray closed circles. (b) The closed and open circles show the dependence of PMMA-S and PMMA-C, respectively.

thickness. Figure 2a shows the fluence dependence of the etch depth of the DM-doped PMMA films, DM(0.15 M)/PMMA-S and DM(0.14 M)/PMMA-C. The DM concentrations were similar while the thicknesses were quite different (see Table 1). Below 700 mJ/cm$^2$, there was no substantial difference between both films except for the thresholds of the swelling: the values were 380 mJ/cm$^2$ for DM(0.14 M)/PMMA-C and 650 mJ/cm$^2$ for DM(0.15 M)/PMMA-S. There was, however, a large difference above 900 mJ/cm$^2$; the etching of about 1 $\mu$m, which is considerable compared with the film thickness, was observed in the case of DM(0.15 M)/PMMA-S, while the swelling of about 11 $\mu$m was observed in the case of DM(0.14 M)/PMMA-C. Figure 2b shows similar results on the neat PMMA films, except for the following points: PMMA-S showed no swelling, and PMMA-C showed a minute etching around 700 mJ/cm$^2$ below the threshold of the swelling. The results in Figure 2a,b strongly suggest that the swelling occurs more easily with an increase in a film thickness.

To investigate the chemical properties of the irradiated films, we developed some films of DM(0.61 M)/PMMA-S after the irradiation. The developer selectively dissolved the irradiated part of the films. For example, DM(0.61 M)/PMMA-S irradiated at 100−200 mJ/cm$^2$ originally swelled before the development, while after the development it was etched to the depth of about 1.4 $\mu$m. Srinivasan *et al.* obtained similar results in the case of neat PMMA irradiated with a 248 nm pulse.[22] In our case, the developer also dissolved the film irradiated at 20 mJ/cm$^2$ where no morphological change was observed before the development. In this case, the film was etched to the depth of 0.9 $\mu$m after the development.

**Transient Absorption Spectra (260−450 nm).** No emission was observed in the wavelength region (260−450 nm), while

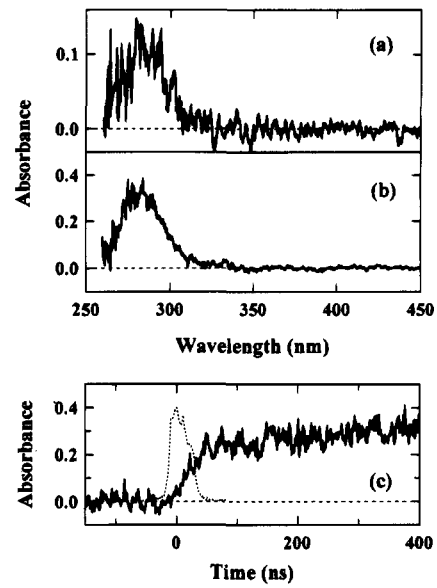


**Figure 3.** Transient absorption spectra of DM(0.61 M)/PMMA-S at 20 mJ/cm$^2$: (a) 0−40 ns and (b) 400−440 ns. The rise-and-decay curve (c) was obtained at 280 nm under the same conditions. The time profile of the laser pulse is also shown in (c).

transient absorption spectra was detected. Figure 3a,b shows the absorption spectra of DM(0.61 M)/PMMA-S irradiated with a 20 mJ/cm$^2$ pulse. The spectrum during the excitation (0−40 ns) agrees with that in the later region (400−440 ns), indicating one transient species with rather long lifetime. We previously obtained a similar spectrum in laser flash photolysis of DM-doped PMMA under the normal excitation conditions and assigned it to the ketene **3**.[20] This was because its decay was very sensitive to the moisture content of the film prior to flash photolysis. Consequently, we conclude here that the spectrum in Figure 3a,b is due to the ketene **3** and that no other transient exists in the time range. The ketene production dynamics is more clearly shown in Figure 3c, where the rise curve consisted of two components, a main fast one and an additional slow one; the ketene was produced almost during the laser pulse, and additionally it was produced after the laser pulse. In a prolonged measurement, the additional slow rise was completed within a few microseconds, and then the ketene existed over the period of the measurement. In other words, no decay was observed up to 40 $\mu$s. It indicates that the ketene in PMMA is rather stable, which is in good agreement with the previous report.[20]

**Transient Absorbance at 248 nm.** The ketene absorption was clearly observed even during the laser pulse, and thus the absorbance at 248 nm should change during the excitation. We have insisted that the measurement of transient absorbance change at excitation wavelength is extremely important,[8] and here the fluence dependence of the time-integrated absorbance at 248 nm is given in Figure 4. The absorbance changed significantly with the laser fluence. The changes of the films were similar; the absorbance decreased with the fluence in the range of several hundred mJ/cm$^2$, and then it increased gradually. To obtain further information on the absorbance change, we also obtained the time-resolved absorbance. The solid lines in Figure 5a−c show the time-resolved absorbance of DM(0.61 M)/PMMA-S at three different fluences. The absorbance decrease became rapid with an increase in the laser fluence. At 740 mJ/cm$^2$, a new increasing component appeared in the later part. This type of the increase in absorbance is commonly observed in laser ablation of a polymer at rather high fluences, and it is assigned to the scattering of the laser pulse by the small fragments or bubbles produced during the ablation.[8,11,12]

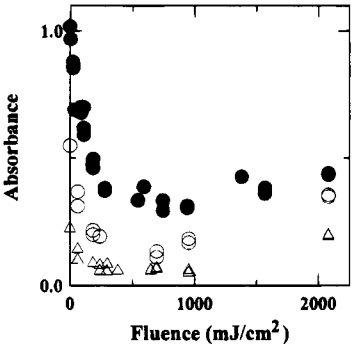


**Figure 4.** Fluence dependence of the time-integrated absorbance of DM(0.15 M)/PMMA-S (△), DM(0.36 M)/PMMA-S (○), and DM(0.61 M)/PMMA-S (●).

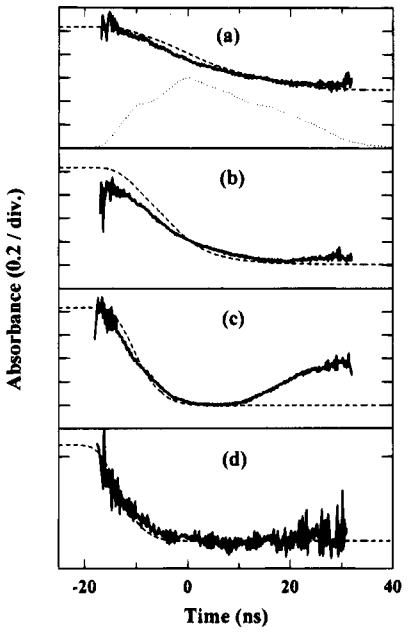


**Figure 5.** Time-resolved absorbance during the laser pulse. The solid lines represent the absorbance obtained experimentally, and the broken lines represent that obtained by the model simulation described in the text. (a) DM(0.61 M)/PMMA-S, 80 mJ/cm²; (b) DM(0.61 M)/PMMA-S, 280 mJ/cm²; (c) DM(0.61 M)/PMMA-S, 740 mJ/cm²; (d) DM(0.15 M)/PMMA-S, 690 mJ/cm². The time profile of the laser pulse is also shown in (a).

Further increase in the laser fluence resulted in the earlier onset of the scattering (not shown in the figure), which is the reason for the increase of the time-integrated absorbance in the high fluence region. The scattering became significant above the following fluences: 1000 mJ/cm² for DM(0.15 M)/PMMA-S, 700 mJ/cm² for DM(0.36 M)/PMMA-S, and 500 mJ/cm² for DM(0.61 M)/PMMA-S.

We have to point out another important feature of the transient absorbance change; the absorbance did not decrease to zero, and in the case of high fluence irradiation, there was the time region where the absorbance remained constant. For example, the absorbance was constant in the middle part of the laser pulse at 740 mJ/cm² (Figure 5c). This feature was more significant in the case of DM(0.15 M)/PMMA-S at 690 mJ/cm² (Figure 5d); the absorbance decreased in the initial part of the laser pulse, and then it was constant in the remainder. We will suggest in the Discussion that the unchanged absorption should arise from the photoabsorption by the ketene.

**Photodecomposition Yield of DM.** We applied the transient absorbance measurement to determine the quantum yield of the photodecomposition of DM. The DM(0.61 M)/PMMA-S film

**SCHEME 2**

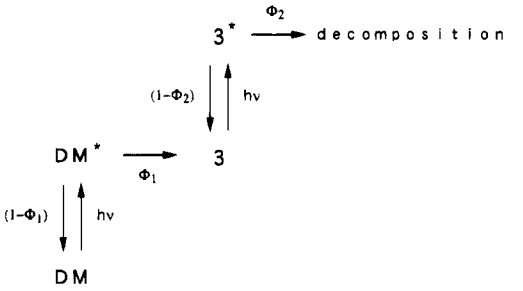


was repetitively irradiated with 2 mJ/cm² pulses, and the transient absorbance of the same position was measured every 10 pulses. The fluence of 2 mJ/cm² was so low that the transient absorbance change during each monitoring pulse was very small. In this case, the transient absorbance measurement practically equals the absorbance measurement done on a spectrophotometer. The measurement allows us to monitor the total concentration of the photodecomposed DM, because we checked by conventional spectrophotometry that there is no substantial photoabsorption by photoproducts of PMMA or DM at 248 nm.[23] The concentration was calculated from the difference between the measured absorbance and the original one, where the extinction coefficient of DM in PMMA at 248 nm ($\epsilon_{DM}$ = 9300 $M^{-1}$ $cm^{-1}$)[24] and the film thickness ($d$ = 1.8 $\mu$m, see Table 1) were used. We simultaneously estimated the total amount of the energy absorbed in the film and plotted the total concentration of the photodecomposed DM against the total absorbed energy. We obtained a value of 0.62 as the yield of the photodecomposition from the slope of the line. This value is a little smaller than that of 1 obtained previously.[20] We conclude that the present value is more accurate one on the basis of the simulation work described in the Discussion.

## 4. Discussion

**Simulation of the Photodecomposition Dynamics of DM.** There are a number of papers on the mechanism of the Wolff rearrangement of *o*-diazo ketones such as DM, and some controversies have been raised.[20,21,25-29] On the basis of laser flash photolysis of six-membered ring *o*-diazo ketones, Tanigaki and Ebbesen concluded that the oxirene intermediates exist as a precursor of the ketenes.[28] They observed two transient species in most cases, and they assigned the first one to the oxirene and the second one to the ketene. Barra *et al.* also conducted laser flash photolysis of *o*-diazonaphthoquinones in acetonitrile with chemical trapping techniques.[29] They observed no thiocarbonyl ylide in the presence of 2-adamantanethione and no carbonyl oxide in the presence of oxygen. Thus, they concluded that α-keto carbenes with lifetimes exceeding a few nanoseconds are not involved as ketene precursors and namely that the Wolff rearrangement is a concerted process on the nanosecond time scale. In the present work on DM in PMMA, only the ketene was detected within and after the laser pulse; no other species was detected. This observation is consistent with the mechanism proposed by Barra *et al.*

To obtain further understanding of the present photodecomposition dynamics during intense excitation, we have done the model simulation described below. Scheme 2 summarizes our model, where an excited state DM* is produced by 248 nm excitation, and it decomposes to the ketene **3** and nitrogen with the yield ($\phi_1$) of 0.62. No precursor of the ketene is presumed, which is consistent with the presumption that the Wolf rearrangement rapidly proceeds in a concerted manner. We presume that the radiationless transition of DM* proceeds with the yield of 0.38 ($1 - \phi_1$), because no appreciable emission of DM was

observed experimentally. We introduce the excitation photon absorption by the ketene, which is characteristic of our model. We have pointed out that the absorbance of the film decreased to a certain value, not zero, and then remained constant during the laser pulse even in the case of high fluence irradiation (see Figure 5c,d). Thus, we assume that the constant absorption arises from the photon absorption by the ketene to which all DM have completely converted. On this assumption, the concentration of the ketene at the constant absorbance is equal to the initial concentration of DM. Then, from the ratio of the constant absorbance to the initial one, we can roughly estimate the extinction coefficient at 248 nm of the ketene ($\epsilon_3$) to be about 1860 $M^{-1}$ $cm^{-1}$, one-fifth of that of DM. In the practical simulation, we changed the value of $\epsilon_3$ around this value to find the best one which reproduces the experimental results.

In our model, the excited state of the ketene **3*** decays through the following two processes: further photodecomposition and radiationless transition. We neglect the hydration of the ketene into **4**, because this reaction is completed in about 1 s and thus hardly proceeds during the nanosecond laser pulse.[20] Kammula *et al.* reported that DM may photodecompose to nitrogen, carbon monoxide, and acetone on the basis of the pyrolysis of DM.[26] They also proposed possible pathways and intermediates in the photodecomposition of the ketene to carbon monoxide and acetone. We do not, however, consider what intermediates are present in the photodecomposition for simplicity; we assume that the photodecomposition of the ketene yields the intermediates which have no absorption at 248 nm. This assumption seems reasonable, because the decomposition should destroy the $\pi$-electron system of the ketene delocalized among five atoms; the system strongly contributes to the absorption of a 248 nm photon. The symbol $\phi_2$ represents the yield of the photodecomposition of the ketene. The value of $\phi_2$ was changed as a parameter in the simulation. The yield of the radiationless transition to the ketene is assumed to be $1 - \phi_2$.

The simulation based on the model was done on a microcomputer in a way similar to that of Sutcliffe and Srinivasan.[30] The laser pulse (about 30 ns), whose time profile was obtained experimentally as in Figure 5a, is split into a sequential train of short rectangular pulses whose pulse width is 20 ps. The film (about 2 $\mu$m) is also split into many continuous thin layers whose thickness is 0.002 $\mu$m. Our simulation is based on Beer's law; when a certain thin layer transmits a rectangular pulse which initially contains $I$ mol/$cm^2$ photons, the amount of the photons absorbed by the layer ($\Delta I$) is calculated by

$$\Delta I = I\{(\ln 10)\epsilon_{DM}[DM] + (\ln 10)\epsilon_3[\mathbf{3}] + \alpha_{PMMA}\}\Delta d \quad (1)$$

where the absorption coefficient of PMMA at 248 nm ($\alpha_{PMMA}$) is 170 $cm^{-1}$ (see Table 1), the layer thickness ($\Delta d$) is $2 \times 10^{-7}$ cm, and the unit of the concentration is M. We presume that $\alpha_{PMMA}$ remains constant during the laser pulse, because the original value of $\alpha_{PMMA}$ is small, and hence we can neglect the generation of the transient states of PMMA. The photodecomposition changes the concentrations of DM and **3** of the layer, and those changes are calculated by

$$\Delta[DM] = -1000(\ln 10)\epsilon_{DM}[DM]\phi_1 I \quad (2)$$

$$\Delta[\mathbf{3}] = 1000(\ln 10)(\epsilon_{DM}[DM]\phi_1 - \epsilon_3[\mathbf{3}]\phi_2)I \quad (3)$$

Note that $\epsilon_3$ and $\phi_2$ are the only parameters in eqs 1−3. The values of the other symbols such as $\epsilon_{DM}$ have been given above. The values of the film thickness and the initial concentration of DM were used as in Table 1.

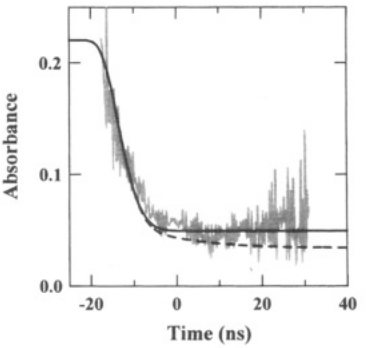


**Figure 6.** Influence of the change in the value of $\phi_2$ on the model simulation. The time-resolved absorbance of DM(0.15 M)/PMMA-S at 690 mJ/$cm^2$ is chosen as an example. The gray solid line represents the experimental result, and the black solid line represents the simulated one with $\phi_2 = 0$. Those are the same as in Figure 5d. The black broken line represents the simulated result with $\phi_2 = 0.1$.

In the simulation, we first calculate the intensity change of the first rectangular pulse at each layer from the surface to the bottom. The absorbance of the film can be calculated from the intensities of the incident and transmitted rectangular pulses. Simultaneously we calculate, at each layer, the amount of the absorbed energy and the concentrations of DM and **3**. Then we do the same calculation successively with the rest of the rectangular pulses. The duration of each rectangular pulse is 20 ps, and thus eqs 1−3 imply that every process in Scheme 2 is rapid enough to complete within 20 ps. It means that the present simulation can deal only with the main fast component of the ketene production mentioned in the Experimental Section. The simulation neglects the slow additional production as an approximation, because it relates to the minor amount of the produced ketene as in Figure 3c.

We have done the simulation with varying the values of the two parameters $\epsilon_3$ and $\phi_2$, and the dashed lines in Figure 5 show the best fit results with $\epsilon_3 = 1700$ $M^{-1}$ $cm^{-1}$ and $\phi_2 = 0$. The obtained value of $\epsilon_3$ agrees with the value estimated roughly above. The simulated curves agree with the measured ones except for two differences, a difference in the early part in Figure 5b and that in the later part in Figure 5c. The former difference is attributed to the uncertainty due to the small signals from the photodiodes mentioned in the Experimental Section, while the latter difference is attributed to the scattering of the laser pulse. The differences are not important, and then the agreement between the measured and simulated curves indicates that our model describes well the photodecomposition dynamics of DM during the laser pulse. The Wolff rearrangement in this model should correspond to the main fast component of the ketene production and is initiated by the photoexcitation of DM. Thus, this reaction may be called "the photochemical Wolff rearrangement". On the other hand, the simulation implies that no electronic excited state such as DM* exists after the laser pulse, and hence the additional slow component is hardly attributed to a photochemical rearrangement. It may arise from the other type of a rearrangement such as a thermal one due to the heat generation by the photoabsorption.

The yield $\phi_2$ is one of the two parameters in our simulation, and we did the simulation with different values of $\phi_2$; when we plot the time-resolved absorbance obtained by the simulation and the experiment, the simulated absorbance deviates from the measured one to zero with an increase in the value of $\phi_2$. Figure 6 shows an example of it, which allows us to conclude that $\phi_2$ is nearly equal to 0, at least smaller than 0.1. It probably indicates that the ketene **3** is not much photoreactive. However, the conclusion is derived on the assumption that the photodecomposition products of the ketene have no absorption at 248

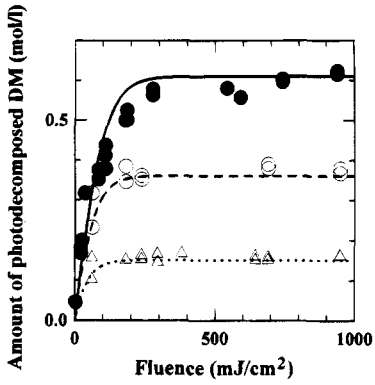


**Figure 7.** Fluence dependence of the amount of the photodecomposed DM per unit volume during the laser pulse. The symbols represent the amounts calculated from the transient absorbance change, and the lines represent those obtained by the simulation. The open triangles and the dotted line show the amounts of DM(0.15 M)/PMMA-S. The open circles and the broken line show the amounts of DM(0.36 M)/PMMA-S. The closed circles and the solid line show the amounts of DM(0.61 M)/PMMA-S.

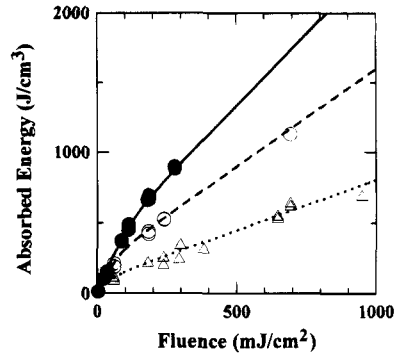


**Figure 8.** Fluence dependence of the absorbed energy per unit volume of the DM-doped films. The symbols represent the energy calculated from the time-integrated absorbance, and the lines represent that obtained by the simulation. The open triangles and the dotted line show the absorbed energy of DM(0.15 M)/PMMA-S. The open circles and the broken line show the absorbed energy of DM(0.36 M)/PMMA-S. The closed circles and the solid line show the absorbed energy of DM(0.61 M)/PMMA-S.

nm. Hence, we cannot fully exclude the presence of the photodecomposition products which give an absorption coefficient similar to that by the original ketene. However, such products seem unlikely when we consider the length of the $\pi$-electron system of them as discussed above, and thus we presume that the ketene does not photodecompose during the laser pulse ($\phi_2 = 0$) in the following discussion.

The simulation with a time step of 20 ps successfully reproduces the absorbance change during the laser pulse, which is consistent with the assumption that "the photochemical Wolff rearrangement" as well as the other processes in Scheme 2 is rapid compared with the time step. Thus, "the photochemical Wolff rearrangement" can be regarded as a reaction in the picosecond time scale. The possible mechanisms of the rearrangement are as follows: (1) it proceeds in a concerted manner and no precursor of the ketene exists, or (2) DM forms a certain precursor such as the carbene or the oxirene, but it decays to yield the ketene within the picosecond time scale. To elucidate the exact mechanism, we have to do a femtosecond pump and probe measurement. Unfortunately, such a measurement is difficult because a white-light continuum in the UV wavelength region (200−300 nm) is hard to obtain at present.

**Dopant Sensitization Mechanism of Laser Ablation.** Now we discuss which is the main process in the dopant sensitization for laser ablation—the photodecomposition of a dopant or the heat generation by the photoabsorption. The value of $\epsilon_3$ has been determined by the simulation, and hence we can calculate the amount of the photodecomposed DM per unit volume from the difference between the initial and the final absorbance during the laser pulse. Note that the amount of the photodecomposed DM is equal to that of the produced nitrogen, which is the driving gas in the photodecomposition mechanism. In the practical calculation, we used the transient absorbance at about 25 ns instead of the final one; the latter is hard to obtain because of the uncertainty mentioned in the Experimental Section. In the case of high-intensity irradiation, the scattering already occurred at 25 ns as in Figure 5c. We then used the minimum absorbance during the laser pulse. Figure 7 shows the results of the calculation; the symbols represent the calculated amounts of DM(0.15 M)/PMMA-S, DM(0.36 M)/PMMA-S, and DM(0.61 M)/PMMA-S. The simulated curves are also shown in the figure. Both the calculated and the simulated amounts are those averaged over the film, from the surface to the bottom; in practice, there are concentration gradients in the films, because the excitation laser intensity decreases with the depth. The simulated amounts agree well with those determined experimentally, except for the slight difference in the case of DM(0.61 M)/PMMA-S.

We can also obtain the absorbed energy per unit volume either by calculation from the time-integrated absorbance or by the simulation (Figure 8). In the calculation, we exclude the time-integrated absorbance affected by the scattering. The absorbed energy obtained in each way is again that averaged over the film. The simulation reproduces the experimental results quite well. However it contains no effect of the scattering, and hence the actual absorbed energy is less than the simulated one at fluences where the scattering is significant.

To discuss the dopant sensitization mechanism of laser ablation, we focus our attention to the fluence range where almost all the DM molecules decompose at the end of the laser pulse. According to Figure 7, the fluences where 90% of DM decompose are as follows: 100 mJ/cm$^2$ for DM(0.15 M)/PMMA-S, 100 mJ/cm$^2$ for DM(0.36 M)/PMMA-S, and 200 mJ/cm$^2$ for DM(0.61 M)/PMMA-S. If the photodecomposition of DM mainly sensitizes ablation, the etch depth of the films should show a saturation tendency above those fluences. In the case of DM(0.61 M)/PMMA-S, considerable morphological changes occurred below and around 200 mJ/cm$^2$, and then the etch depth increased gradually with the fluence (see Figure 1). This increase may be the saturation tendency mentioned above, and then the photodecomposition mechanism seems acceptable. However, the mechanism is clearly inconsistent with the results of DM(0.15 M)/PMMA-S and DM(0.36 M)/PMMA-S. In these cases, no morphological change was observed at 100 mJ/cm$^2$ (see Figures 1 and 2a). Both swelling and etching were observed above them where the amount of the photodecomposed DM is almost constant but that of the absorbed energy increases with an increase in the laser fluence. It is the amount of the absorbed energy, not that of the photodecomposed DM, which governs both swelling and etching. The results of the cast films in Figure 2 give similar information. A neat PMMA film, PMMA-C, swells with an intense irradiation, and its amount of swelling is larger than that of DM(0.14 M)/PMMA-C above 100 mJ/cm$^2$. It indicates that PMMA can swell without a dopant or, in other words, without dopant photodecomposition.

At the present stage, we cannot exclude the possibility that the photodecomposition assists the morphological changes or ablation. On the basis of the discussion above, however, we conclude that the photodecomposition of a dopant is not a main

factor for both swelling and etching. We also conclude that the heat generation by the photoabsorption is the main process which induces ablation. Arnold and Scaiano previously investigated the 266 nm ablation of PMMA doped with 1,1,3,3-tetraphenylacetone, which photodecomposes with excitation at the wavelength.[15] When increasing the laser fluence, they observed the occurrence of a sudden threshold for ablation while the concentrations of the photodecomposition products were building up slowly within the sample. Their report also indicates little or no effect of the photodecomposition on laser ablation and then agrees with our conclusion.

**Thickness Dependence of the Morphological Changes.** The thickness dependence around 2000 mJ/cm$^2$ in Figure 2 gives us useful information on the swelling. In the case of the thin films, the etchings of about 1 $\mu$m were observed. It suggests that the surface layers of a similar thickness are also removed in the case of the thick films, although they showed a considerable swelling. The swelling should originate from the morphological changes of the deeper part of the film. In addition, the results of the development suggest that laser irradiation, even below the threshold of the morphological change, makes PMMA into lower molecular weight ones which can easily dissolve in the developer. When this fragmentation of PMMA has extensively occurred and there still remains enough excess energy, the fragments should leave the film, which results in the etching of the film. In the case of the swelling, however, most of the irradiated PMMA should not get the enough energy to induce appreciable fragmentation and the following ejection of the fragments; only the PMMA in the topmost surface layer should have the enough energy, but those in the deeper part should lack it. Thus, the topmost surface layer leave the film, while the deeper part expands to form a new surface which is higher than the original one; the swelling can be regarded as an incomplete fragmentation and ejection.

It is an inside part of the original film that contributes to the swelling, and thus the swelling depends not only on the thickness but also on the absorption coefficient which governs the penetration depth of a laser pulse. Fukumura *et al.* previously reported, in the case of porphyrin-doped PMMA and other polymers, that the maximum height of the swelling increased with a decrease in the original absorption coefficient.[5] In the present work, similar results were obtained (Figures 1 and 2, Table 1). Those results indicate that the absorption coefficient or the penetration depth also governs the swelling.

There is another interesting feature of the thickness dependence in Figure 2; the thick films showed morphological changes at a low fluence where no change was observed with the thin films. This feature can be explained by different cooling rates of the films, when we accept the thermal nature of laser ablation. Furutani *et al.* recently investigated the substrate dependence of laser ablation by time-resolved interference measurement.[6] They prepared biphenyl-doped PMMA films on a quartz or PMMA substrate and monitored the surface displacement of the films irradiated with a 248 nm pulse (30 ns) below the ablation thresholds. The surfaces of both films expanded to a similar height within several tens of nanoseconds after the irradiation, while the height of the film on a quartz substrate returned to the original one much faster than that on a PMMA substrate. They attributed the expansion to transient heating and then the different decay times to the different thermal conductivities of the substrates. Our results can be explained in a similar way. The present thick films correspond to the film on a PMMA substrate, and the heat in them remains longer than that in the thin films. It assists the thermal decomposition to proceed in the thick films and then results in their lower thresholds. Note that this explanation contains no effect of the chemical nature of a dopant; in other words, it is only based on the thermal processes in a polymer film.

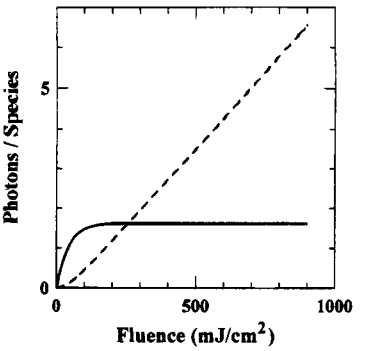


**Figure 9.** Simulated number of the photons absorbed by the ground state (solid line) and that by the ketene (broken line) in the case of DM(0.15 M)/PMMA-S.

**Cyclic Multiphotonic Absorption by the Ketene Leading to Heat Generation.** Finally, on the assumption that the ketene is only the intermediate which absorbs 248 nm photons, we discuss the mechanism of the energy absorption and its dissipation resulting in ablation. Our model simulation allows us to estimate the number of the photons absorbed by the ground state and that by the ketene. Figure 9 shows those numbers of DM(0.15 M)/PMMA-S at fluences below 900 mJ/cm$^2$ where we can neglect the scattering of the laser pulse. The obtained values are those averaged over the all DM molecules in the irradiated part. The ground state absorbs at most 1.6 photons before DM molecules are photodecomposed, while the ketene can absorb more photons with an increase in the laser fluence; for example, at 900 mJ/cm$^2$, it abosrbs 6.6 photons.[31] In the case of DM(0.36 M)/PMMA-S and DM(0.61 M)/PMMA-S, we also obtained the relations similar to that in Figure 9; namely, the number of the absorbed photons at each fluence did not depend distinctly on the DM concentration. On the other hand, the fluence where we observe the same etch depth decreased with an increase in the DM concentration (see Figures 1 and 2a). Thus, the higher the concentration of DM, the less the photon absorption by the ketene contributes to a morphological change. However, as in Figure 9, the ketene absorbs more photons than the ground state in a high fluence region even in the case of a high DM concentration. We have come to the following tentative conclusion: the ketene should repeatedly absorb 248 nm photons, and it should practically contribute to obtain the energy to induce ablation, especially in a high fluence region.

The multiphotonic absorption by a dopant was previously observed in the case of 351 nm ablation of polystyrene doped with anthracene[7] and 248 nm ablation of PMMA doped with pyrene or biphenyl.[8] In each case, we obtained the experimental evidence that a dopant absorbs more than 10 photons during the laser pulse above the ablation threshold. To explain such considerable multiphotonic absorption and the resulting ablation, we have proposed "cyclic multiphotonic absorption" by transient states such as the lowest singlet state ($S_1$), the lowest triplet state ($T_1$), cation and anion.[7-9] The higher excited states ($S_n$, $T_n$, and excited states of ions) generated by the absorption of excitation photons generally have a lifetime extremely shorter than the duration of a nanosecond laser pulse. The quite rapid relaxation to the initial transient states allows the cyclic absorption of excitation photons. On the other hand, the relaxation consists of the internal conversion in the dopant and the intermolecular vibrational energy transfer from the dopant to the surrounding matrix polymer. The matrix polymer is

heated repeatedly during the multiphotonic absorption; the dopant works as a "molecular converter" of the absorbed photon energy into the heat energy. The heated polymer thermally decomposes, which results in ablation. Note that the ground state or the reaction intermediates also can contribute to the cyclic absorption if their excited states relax to the initial states rapidly enough.

This mechanism explains not only the ablation of aromatic-doped polymers but also the ablation of DM-doped PMMA. In the present case, the species which contributes to the cyclic absorption should be the ketene **3**. However, it still remains unclear whether the ketene is intact during such multiphotonic absorption, even though the absorbed energy can be released to the matrix polymer PMMA. To make clear this point, we have to measure the transient absorption spectrum during the laser pulse at a high fluence where the ketene is expected to absorb several 248 nm photons. However, such measurement is difficult with our streak camera system, because the signal due to the scattered laser pulse is stronger than the monitoring light in the wavelength region of 250−300 nm at such a high fluence. Thus, we can only stress the following point: the cyclic multiphotonic absorption by the ketene is quite consistent with the present results.

## 5. Conclusion

We have shown the thermal nature of dopant sensitized ablation. We conclude that photodecomposition of a dopant has little or no effect on laser ablation. The thickness dependence of the morphological change allows us to obtain the picture of the swelling; an intense irradiation makes PMMA decompose into lower molecular weight ones, and the topmost surface layer is removed while the deeper part is left and swollen because of the lack of enough energy. We have considered the photodecomposition dynamics of DM; the Wolff rearrangement initiated by the photoabsorption is considered to proceed on the picosecond time scale. The cyclic multiphotonic absorption by the ketene is quite consistent with the experimental results.

**Acknowledgment.** This work was partly supported by a Grant-in-Aid on Priority-Area-Research "Photoreaction Dynamics" from the Japanese Ministry of Education, Science and Culture (06239101). We are grateful both to ANELVA Corp. for the use of the excimer laser and to Dr. M. Takagi of the Institute of Laser Engineering in Osaka University for the use of the depth profiler. We are also grateful to Prof. M. A. Winnik for valuable discussions.

## References and Notes

(1) Ashby, C. I. H. In *Thin Film Processes II*; Vossen, J. L., Kern, W., Eds.; Academic Press: San Diego, 1991; pp 783−856.
(2) Srinivasan, R.; Braren, B. *Chem. Rev.* **1989**, *89*, 1303−1316.
(3) Chuang, T. J.; Hiraoka, H.; Mödl, A. *Appl. Phys. A* **1988**, *45*, 277−288.
(4) Masuhara, H.; Hiraoka, H.; Domen, K. *Macromolecules* **1987**, *20*, 450−452.
(5) Fukumura, H.; Mibuka, N.; Eura, S.; Masuhara, H. *Appl. Phys. A* **1991**, *53*, 255−259.
(6) (a) Furutani, H.; Fukumura, H.; Masuhara, H. The 6th Symposium on Unconventional Photoactive Solids, Leuven, 1993; Abstract pp 124−125. (b) Fukumura, H.; Furutani, H.; Masuhara, H. PME Symposium, Kawasaki, 1993; Abstract pp 30−33. (c) Furutani, H.; Fukumura, H.; Masuhara, H. *Appl. Phys. Lett.* **1994**, *65*, 3413−3415.
(7) Fukumura, H.; Mibuka, N.; Eura, S.; Masuhara, H.; Nishi, N. *J. Phys. Chem.* **1993**, *97*, 13761−13766.
(8) Fujiwara, H.; Hayashi, T.; Fukumura, H.; Masuhara, H. *Appl. Phys. Lett.* **1994**, *64*, 2451−2453.
(9) Fukumura, H.; Masuhara, H. *Chem. Phys. Lett.* **1994**, *221*, 373−378.
(10) Wen, X.; Tolbert, W. A.; Dlott, D. D. *Chem. Phys. Lett.* **1992**, *192*, 315−320.
(11) Chen, S.; Lee, I.-Y. S.; Tolbert, W. A.; Wen, X.; Dlott, D. D. *J. Phys. Chem.* **1992**, *96*, 7178−7186.
(12) Lee, I.-Y. S.; Wen, X.; Tolbert, W. A.; Dlott, D. D.; Doxtader, M.; Arnold, D. R. *J. Appl. Phys.* **1992**, *72*, 2440−2448.
(13) Wen, X.; Tolbert, W. A.; Dlott, D. D. *J. Chem. Phys.* **1993**, *99*, 4140−4151.
(14) Wen, X.; Hare, D. E.; Dlott, D. D. *Appl. Phys. Lett.* **1994**, *64*, 184−186.
(15) Arnold, B. R.; Scaiano, J. C. *Macromolecules* **1992**, *25*, 1582−1587.
(16) Srinivasan, R.; Braren, B.; Dreyfus, R. W.; Hadel, L.; Seeger, D. E. *J. Opt. Soc. Am. B* **1986**, *3*, 785−791.
(17) Srinivasan, R.; Braren, B. *Appl. Phys. A* **1988**, *45*, 289−292.
(18) Bolle, M.; Luther, K.; Troe, J.; Ihlemann, J.; Gerhardt, H. *Appl. Surf. Sci.* **1990**, *46*, 279−283.
(19) Lippert, Th.; Wokaun, A.; Stebani, J.; Nuyken, O.; Ihlemann, J. *Angew. Makromol. Chem.* **1993**, *213*, 127−155.
(20) Winnik, M. A.; Wang, F.; Nivaggioli, T.; Hruska, Z.; Fukumura, H.; Masuhara, H. *J. Am. Chem. Soc.* **1991**, *113*, 9702−9704.
(21) Andraos, J.; Chiang, Y.; Huang, C.-G.; Kresge, A. J.; Scaiano, J. C. *J. Am. Chem. Soc.* **1993**, *115*, 10605−10610.
(22) Srinivasan, R.; Braren, B.; Casey, K. G. *J. Appl. Phys.* **1990**, *68*, 1842−1847.
(23) We measured the absorption spectrum around 248 nm of DM(0.15 M)/PMMA-S after 300 mJ/cm$^2$ irradiation, and the spectrum was similar to that of PMMA-S.
(24) This value was obtained by measuring the absorbance of the DM-doped PMMA film whose thickness and concentration of DM were known.
(25) Zeller, K.-P. *J. Chem. Soc., Chem. Commun.* **1975**, 317−318.
(26) Kammula, S. L.; Tracer, H. L.; Shevlin, P. B.; Jones, M., Jr. *J. Org. Chem.* **1977**, *42*, 2931−2932.
(27) Shibata, T.; Koseki, K.; Yamaoka, T.; Yoshizawa, M.; Uchiki, H.; Kobayashi, T. *J. Phys. Chem.* **1988**, *92*, 6269−6272.
(28) Tanigaki, K.; Ebbesen, T. W. *J. Phys. Chem.* **1989**, *93*, 4531−4536.
(29) Barra, M.; Fisher, T. A.; Cernigliaro, G. J.; Sinta, R.; Scaiano, J. C. *J. Am. Chem. Soc.* **1992**, *114*, 2630−2634.
(30) Sutcliffe, E.; Srinivasan, R. *J. Appl. Phys.* **1986**, *60*, 3315−3322.
(31) The number of the absorbed photons at 900 mJ/cm$^2$ is estimated to be 4.8 in the case of $\phi_2 = 0.1$, the value of which is the upper limit as concluded from Figure 6; the presumption of $\phi_2 = 0$ is not crucial for the suggestion by the simulation that the ketene can absorb several 248 nm photons.

JP941862N